doi: 10.4149/gpb_2022032

The role and mechanism of NDST1/NULP1 regulating right ventricular hypertrophy in hypoxic pulmonary hypertension

Haixia Sun[1,*], Junling Liu[2,*], Yuxin Su[1], Fang Li[1], Mingyue Zhang[1], Jia Li[1] and Meiling Song[3]

[1] *Qinghai Provincial People's Hospital, Xining, Qinghai, China*
[2] *Xining Hospital of Traditional Chinese Medicine, Xining, Qinghai, China*
[3] *Medical College of Qinghai University, Xining, Qinghai, China*

Abstract. Hypoxia leads to hypoxic pulmonary hypertension (HPH), causing right ventricular hypertrophy (RVH). RVH becomes a significant and nonnegligible public health issue in the world. In our study, we successfully established the HPH rat model and found that RVH happened in HPH, and then we observed an increased inflammation response in the heart tissue of HPH-induced RVH rats. Moreover, increased N-deacetylase-N-sulfotransferase-1 (NDST1) and decreased nuclear localized protein 1 (NULP1) were found in the heart tissue of HPH-induced RVH rats. An *in vitro* cell experiment showed that inhibition of NDST1 expression enhanced cell viability, reduced cell apoptosis, alleviated cardiomyocyte hypertrophy, decreased inflammation and increased phosphorylated AKT level, however, over-expression of NDST1 had opposite effects on these aspects. NULP1 reversed the effects of NDST1 on these regulations. Finally, we found that up-regulated NDST1 reduced NULP1 expression and down-regulated NDST1 increased NULP1 expression. Our study confirmed that inhibition of the NDST1/NULP1 pathway might contribute to the attenuation of HPH-induced RVH, and the mechanism may be related to the reduction of inflammation, cardiomyocyte apoptosis, and AKT phosphorylation.

Key words: Hypoxic pulmonary hypertension — Right ventricular hypertrophy — NDST1/NULP1 — AKT — Cardiomyocyte hypertrophy

Abbreviations: ANP, atrial natriuretic peptide; BNP, brain natriuretic peptide; HPH, hypoxic pulmonary hypertension; MPAP, mean pulmonary artery pressure; Myh7, myosin heavy chain 7; NDST1, N-deacetylase-N-sulfotransferase-1; NFAT3, nuclear factor of activated T cells 4; NULP1, nuclear localized protein 1; RHW/BW, right heart weight/body weight; RVH, right ventricular hypertrophy; RVH, right ventricular hypertrophy.

Introduction

Hypoxic pulmonary hypertension (HPH) is a common complication of chronic pulmonary diseases, such as chronic obstructive pulmonary disease, interstitial pulmonary disease, and chronic pulmonary heart disease (Zeng et al. 2017). Remarkably HPH contributed to the progress of right ventricular hypertrophy (RVH) and increased mortality (Zangiabadi et al. 2014). Therefore, RVH led by HPH is a significant nonnegligible public health issue.

NULP1 (nuclear localized protein 1) is a basic helix-loop-helix transcription factor that plays an important role in embryonic development (Steen and Lindholm 2008). NULP1 expression is highly enriched in a healthy adult heart but significantly reduced in heart failure after ischemia (Cai et al. 2006; Lachtermacher et al. 2010). The studies conducted up to date have demonstrated that NULP1 is a negative

* These authors contributed equally to this work.
Electronic supplementary material. The online version of this article (doi: 10.4149/gpb_2022032) contains Supplementary material.
Correspondence to: Hiaxia Sun, Qinghai Provincial People's Hospital, 2 Gonghe Road, Xining Qinghai, 810007, China
E-mail: tbb0302@sina.com

regulator of cardiac hypertrophy, and the mechanism underlying this effect was related to NFAT3 (nuclear factor of activated T cells 4, NFATc4) signaling under hypertrophic stress (Zhang et al. 2020).

N-deacetylase-N-sulfotransferase-1 (NDST1), one of the heparan sulfate modifying enzymes, is abundantly and ubiquitously expressed in all embryonic and adult tissues in vertebrates. It has been shown that NDST1 deficiency contributes to decreasing the invasion of inflammatory cells (Wang et al. 2005) and improving acute antigen-induced nephritis and allergic airway disease (Rops et al. 2014). Moreover, another study showed that loss of NDST1 decreased the intima/media ratio in adult mice with femoral artery injury. However, the role of NULP1 and NDST1 in RVH induced by HPH is still unclear, and the underlying mechanism is also poorly understood. We speculated that NDST1/NULP1 may be involved in this process.

Therefore, in our study, a rat model of HPH was established, and we aimed to explore the role of NULP1 and NDST1 in RVH induced by HPH, and documented evidence using *in vitro* experimental approaches.

Materials and Methods

Animals and establishment of HPH model

24 Sprague-Dawley male rats (SPF grade, 3 weeks) were purchased from Chengdu Dossy Experimental Animals Co., LTD. (Chengdu, Sichuan). Ethics approval was granted from the Medical Ethics Committee of Qinghai Provincial People's Hospital. Rats were placed in an environment with freely available food and water, 25 ± 1°C, with relative humidity 50–60%, and light/darkness for 12 h circulation. 24 rats were randomly and equally divided into four groups (n = 6 rats/group): (1) NG-21d, normoxia group, rats were regularly fed for 21 days; (2) NG-28d, normoxia group, rats were regularly fed for 28 days; (3) HG-21d, hypoxia group, rats were exposed to a concentration of 10 ± 0.5% O_2 for 8 h every day, 6 days a week with a total periods 21 days; (4) HG-28d, hypoxia group, rats were exposed to a concentration of 10 ± 0.5% O_2 for 8 h every day, 6 days a week with a total periods 28 days.

Mean pulmonary artery pressure (MPAP) test

Rats were intraperitoneally injected with 50 mg/kg pentobarbital sodium, and then endotracheal intubation connected with a ventilator was performed to assist respiration (0.018 ml/g body wt (BW) and 130 cycles/min). A micro-TIP pressure catheter (SP-1000; Millar Instruments, Houston, TX) was directly punctured into the main pulmonary artery through the right ventricle with a thoracotomy approach. MPAP data were recorded with a Powerlab system.

Right heart hypertrophy measurement

Before the MPAP test, BW was measured. After the MPAP test, heart tissues were harvested after exsanguination. Right ventricle (RV) and left ventricle and septum (LV+S) were separated and immediately weighed. The right heart index (RHW/BW) was determined by the mass ratio of the right heart/body, and RVH index (right ventricular hypertrophy index) was determined by the mass ratio of RV/(LV+S).

HE staining

The HE staining was performed following standard procedures (Cardiff et al. 2014). In brief, RV tissue sections were dewaxed to water and stained with hematoxylin solution and eosin solution in turn. The sections were observed by routine optical microscopy.

Cell culture and treatment

H9c2 cardiomyoblast cell lines were obtained from the Shanghai Cell Bank (Shanghai, China). First, the H9c2 cardiomyoblast cells were resuscitated by maintaining in a DMEM medium that contained 10% fetal bovine serum (FBS), 100 U/ml penicillin, and 100 g/ml streptomycin and culturing at 37°C with 5% CO_2 in a humidified incubator. Hypoxia H9c2 cells were established in an incubator containing 94% N_2, 5% CO_2, and 1% O_2 for 24 h. Before the hypoxia cell model establish, Lipofectamine 3000 transfection reagent was used for the transient transfection in H9c2 cells (1.0×10^5 cells/well), including NDST1 siRNA (si-NDST1) or NDST1 overexpression vector (pcDNA-NDST1), the transient transfection of NULP1 siRNA (si-NULP1) or NULP1 overexpression vector (pcDNA-NULP1). In brief, for gene overexpression, pcDNA (2 μg/well) or pc-NC (2 μg/well) and transfection reagent (12 μl/well) was diluted in 150 μl of serum-free Opti-MEM (Gibco, USA) for 5 min, respectively. For gene silencing, siRNA (75 pmol/well) or si-NC (75 pmol/well) and transfection reagent (7.5 μl/well) were diluted in 100 μl of serum-free Opti-MEM for 5 min, respectively. Then, the diluted transfection reagent and plasmid/siRNA were mixed and incubated at 37°C for 30 min. The transfection mixture was added to the cell culture medium and mixed. The cell culture medium was replaced with fresh DMEM containing 10% FBS after 6 h of transfection, and the culture was continued for 24 h. The transfection efficiency was tested with Western blotting. The specific groupings were: (1) Normoxia group (NG), (2) Hypoxia group (HG), (3) HG+si-NDST1, (4) HG+pcDNA-NDST1, (5) HG+si-NDST1+si-NULP1, (6) HG+pcDNA-NDST1+pcDNA-NULP1. si-NDST1 (sc-270039) and si-NULP1 (sc-270039) were purchased from Santa Cruz Biotechnology (USA). PcDNA3.1 vector was purchased

from Invitrogen (USA) and the fragments were connected to the pcDNA3.1 vector to construct pcDNA3.1-NDST1 (pcDNA-NDST1) and pcDNA3.1- NULP1 (pcDNA-NULP1). The empty pcDNA-3.1 vector and si-NC served as the control.

CCK-8 assay

Cardiomyocyte viability was indirectly observed by the CCK-8 assay. The cells were plated in 96-well plates at a density of 3×10^3 cells *per* well. 24 h later, the cells were transfected with the indicated pcDNAs or siRNAs under normal or hypoxia conditions. After 48 h, the cells were incubated at 37°C for 1 h in the 100 μl fresh culture medium containing 10% CCK-8 reagent (DoJinDo Laboratory, Japan). Then, an automatic spectrometer (Multimode Reader, PerkinElmer, USA) was used to measure the absorbance in the well at 450 nm.

Rhodamine-phalloidin and DAPI staining

The rhodamine-phalloidin and DAPI staining were performed as previously described (Gourlay et al. 2004). In brief, after treatment, cells were washed. Then cells were fixed with 3.7% formaldehyde and stained with phalloidin-rhodamine. DAPI nuclei staining was performed after phalloidin-rhodamine staining. A Zeiss Observer Z1 microscope (Carl Zeiss, Germany) was used to observe the staining results.

Flow cytometric analysis of apoptosis

An apoptosis detection kit (Nanjing KeyGen Biotech Co., Ltd.) was used to detect cell apoptosis. After that, Annexin V-fluorescein isothiocyanate and propidium iodide were added and cultured for 15 min at room temperature and darkness. Apoptosis results were observed by a BD flow cytometer and analyzed by a FlowJo software version 7.6.5.

Western blot

The total proteins of RV tissue and cells were extracted with the frozen RIPA lysis buffer and quantified by the bicinchoninic acid (BCA) method. The protein samples were separated by 10% PAGE electrophoresis and transferred to PVDF membrane. Then 5% skim milk powder was cultured with samples for 2 h at room temperature. After that, the primary antibodies (ANP, BNP, Myh7, AKT and P-Akt antibodies were purchased from Abcam in the UK) were added and incubated overnight at 4°C. Then the secondary antibodies were added and cultured at room temperature for 2 h. After development with ECL solution, ImageJ software was used to analyze the result. Beta-actin was used to normalize protein levels in this experiment.

ELISA

Heart tissue and H9c2 cells were collected. The IL-6 and TNF-α levels were assayed by ELISA kits according to the manufacturer's protocols. The IL-6 and TNF-α ELISA kits both were purchased from shanghai Enzyme-linked Biotechnology (Shanghai, China).

Statistical analysis

SPSS 18.0 software was used to analyze the results. Data were expressed as mean ± SD. Statistical analysis was performed by one-way ANOVA with Tukey's test for multiple comparisons. Differences were considered statistically significant when $p < 0.05$.

Result

Construction of the HPH-induced RVH rat model

First, we aimed to verify the successful establishment of the HPH-induced RVH rat model. As shown in Figure 1A, compared to the NG group, the MPAP levels were significantly augmented in the HG group at 21 days and 28 days. Significant elevation in RHW/BW and RVH index was observed in HG-21d and HG-28d. Furthermore, as shown in Figure 1B, HE staining showed that the heart structure of the NG group was normal at 21 days and 28 days, with clear and complete structures and no evident lesions. The HG group showed a small amount of myocardial fiber necrosis at 21 days, and the severity of the heart lesions was aggravated at 28 days. ANP, BNP and Myh7 genes have been reported to serve as hallmarks in the development of cardiac hypertrophy (Tyser et al. 2016; Li et al. 2017; Fang et al. 2018). Hypoxic treatment with 21 days and 28 days both caused an increase in ANP, BNP, and Myh7 mRNAs levels and proteins levels in HG, indicating hypoxic-treatment induced right ventricular hypertrophy (Fig. 1C). Moreover, the Myh7 mRNA level in HG-28d was higher than HG-21d. Our results revealed that the HPH-induced RVH rat was successfully modeled, and the severity of RVH became worse with time hypoxic treatment induced.

Effect of HPH-induced RVH on the inflammation of heart tissue

To further explore the effects HPH-induced RVH caused, the inflammatory factors in the heart tissue were carried out. 21-

and 28-day hypoxic treatment both resulted in the increased IL-6 and TNF-α levels in the heart tissue comparing to NG groups (Fig. 2). Further, IL-6 and TNF-α levels in the heart tissue showed increasing trends as the hypoxic-treated days increased. Those data suggested that HPH-induced RVH caused inflammation in heart tissue.

RVH induced by HPH changed the expression of NDST1/NULP1 in the right ventricle

To elucidate the possible mechanism of NDST1/NULP1 in RVH induced by HPH, we investigated the mRNAs and protein expressions of NDST1 and NULP1 in RV. There

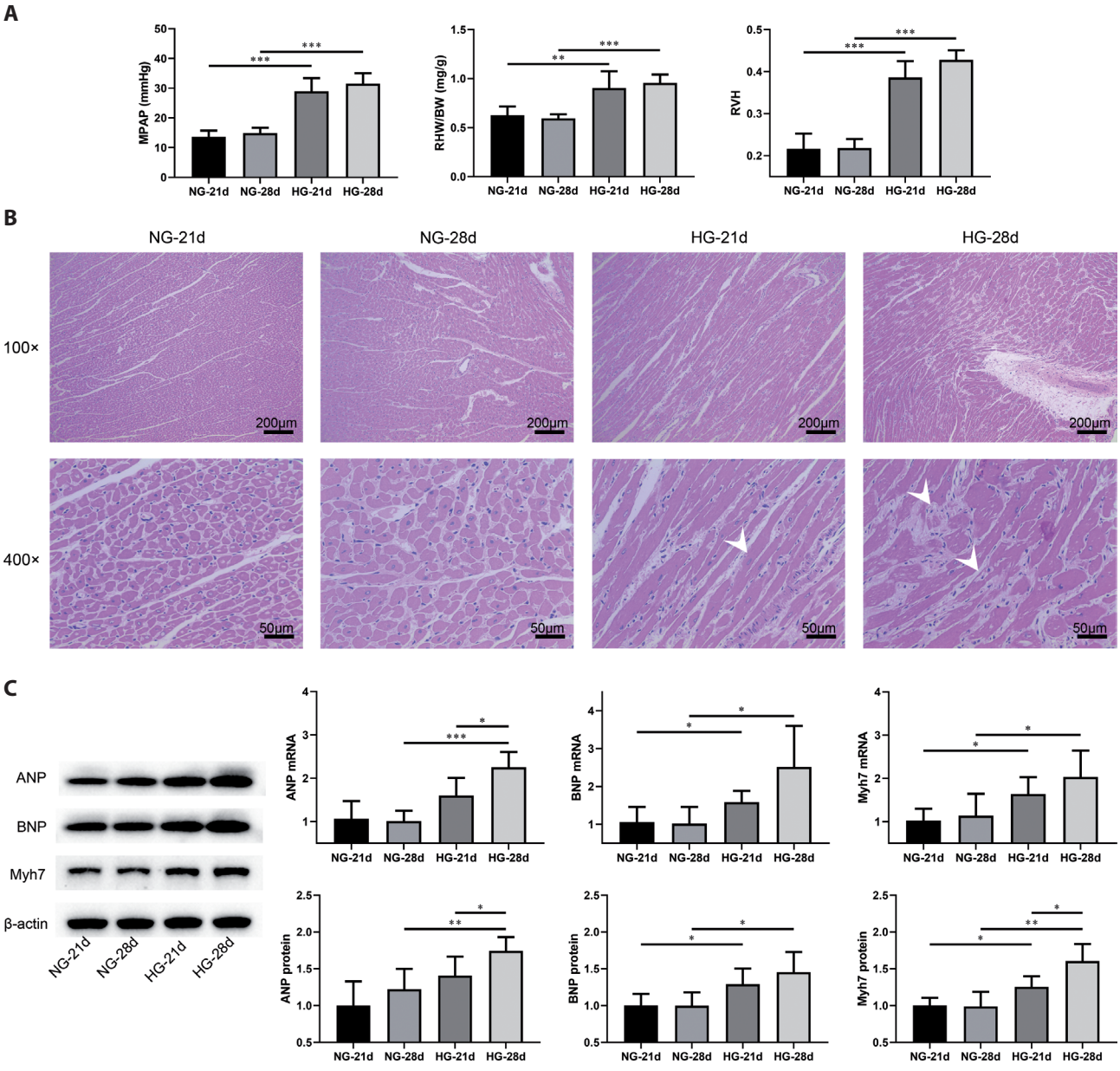

Figure 1. Hypoxic pulmonary hypertension-induced right ventricular hypertrophy rat model. **A.** Heart function indexes: MPAP (mean pulmonary artery pressure), RHW/BW (right heart weight/body weight) index and RVH (right ventricular hypertrophy) index. **B.** HE staining. White arrows: myocardial fiber necrosis. **C.** Q-PCR and Western blot detected for cardiac hypertrophy markers, including ANP, BNP, and Myh7. * $p < 0.05$, ** $p < 0.01$, *** $p < 0.001$. NG-21d, normoxia group, rats were regularly fed for 21 days; NG-28d, normoxia group, rats were regularly fed for 28 days; HG-21d, hypoxia group, rats were exposed to a concentration of 10 ± 0.5% O_2 for 8 h every day, 6 days a week with a total periods 21 days; HG-28d, hypoxia group, rats were exposed to a concentration of 10 ± 0.5% O_2 for 8 h every day, 6 days a week with a total periods 28 days.

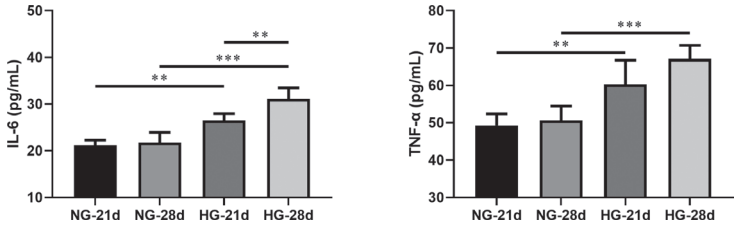

Figure 2. The inflammatory factors IL-6 (**A**) and TNF-α (**B**) were detected by ELISA in the heart tissue. ** $p < 0.01$, *** $p < 0.001$. For abbreviations, see Figure 1.

was an increase in the NDST1 expression and a decrease in the NULP1 expression in HG compared to NG, which suggested that NDST1 activation and NULP1 inhibition were involved in the development of HPH-induced RVH (Fig. 3). Moreover, compared to HG-21d, the change of NDST1 and NULP1 in HG-28d had an aggravated tendency with time. These data prompted us to ask one question: whether cardiac hypertrophy led by hypoxia can be modified after suppressing the alterations of NDST1 or NULP1 expression.

NDST1/NULP1 could regulate hypertrophy in hypoxia-induced H9C2 cells

To validate our hypothesis, we designed an *in vitro* cell experiment. First, we verified that H9C2 cells were successfully transfected with si-NDST1, pcDNA-NDST1, si-NULP1 and pcDNA-NULP1 (Supplementary Materials, Fig. S1). As shown in Figure 4A, the decreased NULP1 level was found in the hypoxia-induced H9C2 cells and NDST1 modulated NULP1 protein expression negatively. Muscle actin has been demonstrated to be a molecular marker for pressure-overload hypertrophy, so we examined the expression of muscle actin in the right ventricle. Under hypoxic stress, muscle actin expression was significantly increased relative to those in normoxia treatment (Fig. 4B). With si-NDST1 treatment, increased muscle actin expression was inhibited in hypoxia-induced H9C2 cells, and adding si-NULP1 prevented that improvement of si-NDST1 in muscle actin expression. In addition, pcDNA-NDST1 promoted an increase in muscle actin expression in hypoxia-induced H9C2 cells, and we observed there was again a trend towards improved performance of increased muscle actin expression with pcDNA-NULP1 treatment in H9C2 cells treated with pcDNA-NDST1 and hypoxia. Those results showed that NDST1/NULP1 participated in the regulation of hypertrophy in hypoxia-induced H9C2 cells. To further investigate the effect and mechanism of NDST1/NULP1 on hypertrophy, other hypertrophic markers were detected by Western Blot in H9C2 cells. As shown in Figure 4C, compared to normoxia treatment, there were significant increases in ANP, BNP, and Myh7 protein expressions with hypoxia treatment. With si-NDST1 treatment, ANP, BNP, and Myh7 protein expressions were inhibited in hypoxia-induced H9C2 cells and the decreased Myh7 expres-

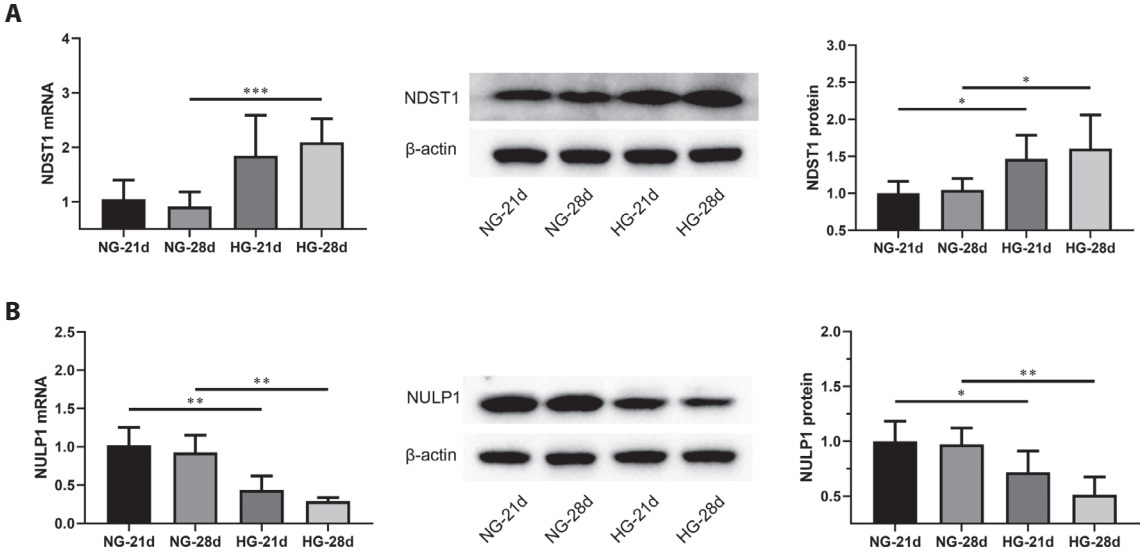

Figure 3. Hypoxic pulmonary hypertension-induced right ventricular hypertrophy changed the expression of NDST1 (**A**) and NULP1 (**B**) in the right ventricle. * $p < 0.05$, ** $p < 0.01$, *** $p < 0.001$. For abbreviations, see Figure 1.

sions led by si-NDST1 were prevented by si-NULP1. With pcDNA-NDST1 treatment, increased proteins expressions of ANP and BNP were up-related in hypoxia-induced H9C2 cells, and those changes were inhibited by pcDNA-NULP1. Those results showed that NDST1/NULP1 could regulate hypertrophy in cardiomyocytes.

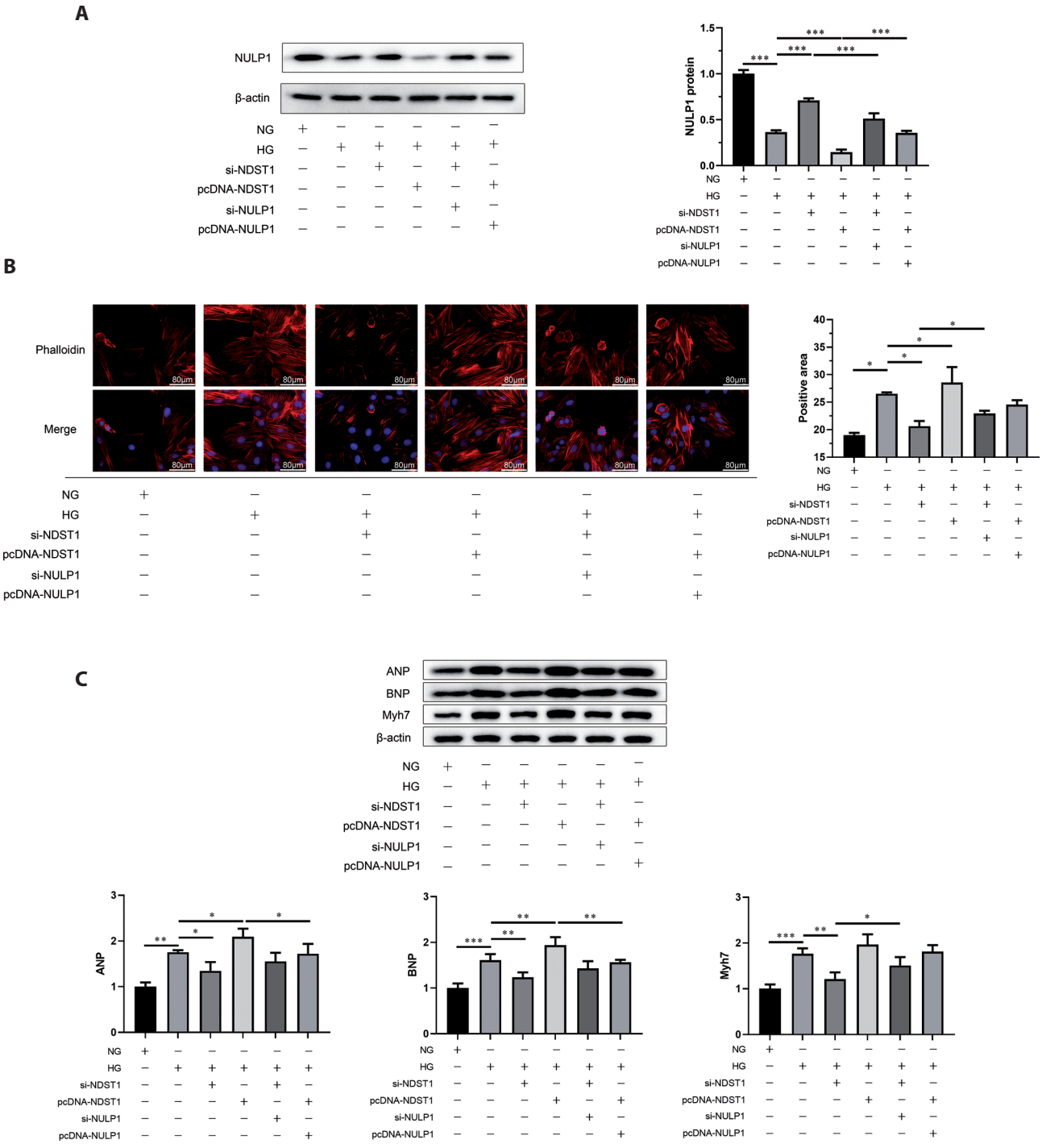

Figure 4. NDST1/NULP1 could regulate hypertrophy in hypoxia-induced H9C2 cells. **A.** Western blot detected for NULP1 expression. **B.** Rhodamine-phalloidin and DAPI staining. Red denotes muscle actin and blue denotes cell nuclei. **C.** Western blot detected for cardiac hypertrophy markers, including ANP, BNP, and Myh7. * $p < 0.05$, ** $p < 0.01$, *** $p < 0.001$. For abbreviations, see Figure 1.

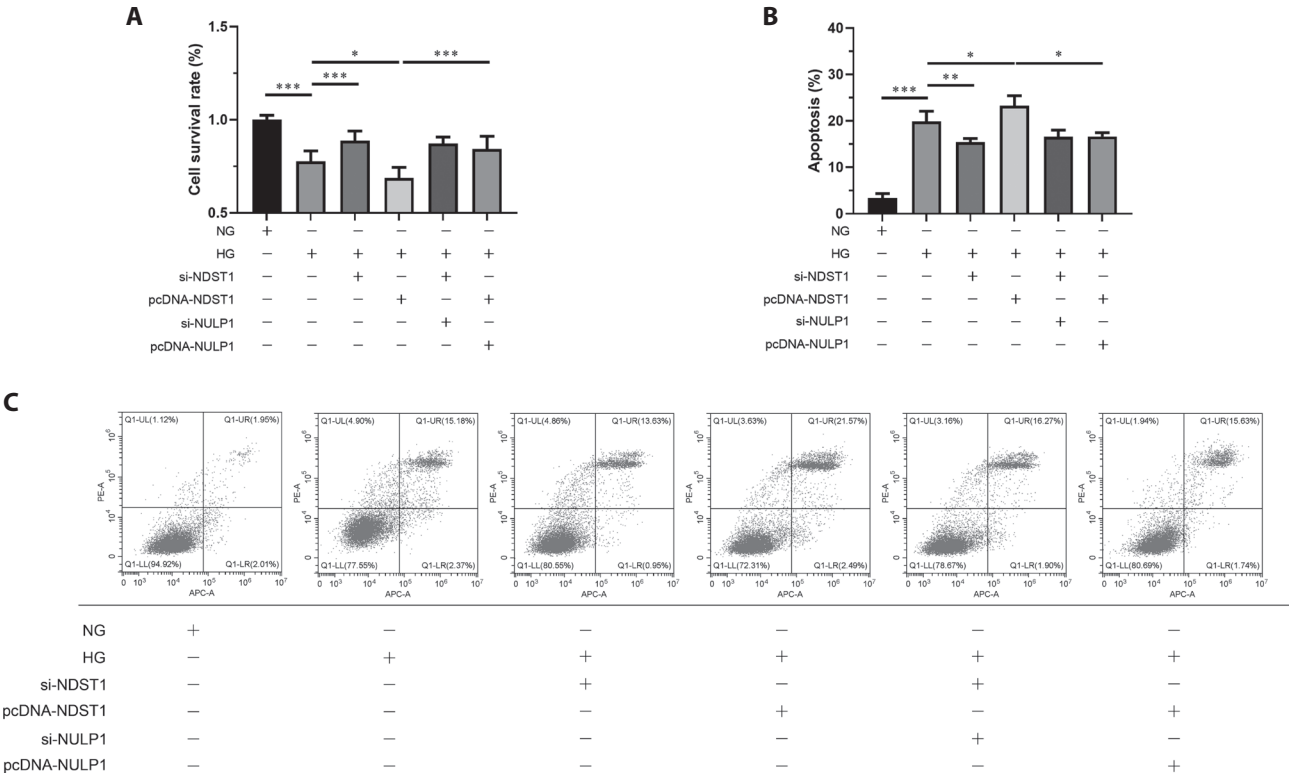

Figure 5. NDST1/NULP1 regulated the cell apoptosis and cell viability in hypoxia-induced H9C2 cells. **A.** CCK-8 detected for cell viability. **B,C.** Apoptosis results of flow cytometry. * $p < 0.05$, ** $p < 0.01$, *** $p < 0.001$. For abbreviations, see Figure 1.

NDST1/NULP1 regulated the cell apoptosis and cell viability in hypoxia-induced H9C2 cells

Hypoxia treatment led to increased cell apoptosis and decreased cell viability (Fig. 5). si-NDST1 reduced cell apoptosis and enhanced cell viability in hypoxia-induced H9C2 cells and pcDNA-NDST1 caused opposite results. Similarly, regulation of NULP1 expression inhibited the effect of pcDNA-NDST1 on cell apoptosis and cell viability in hypoxia-induced H9C2 cells.

NDST1/NULP1 regulated the phosphorylation of AKT and the secretion of inflammatory factors in hypoxia-induced H9C2 cells. To explore the regulatory effect of NDST1/NULP1 on the AKT pathway in hypoxia-induced H9C2 cells, we performed a Western Blot assay to detect phosphorylated AKT. As shown in Figure 6A, hypoxia treatment activated phosphorylated AKT. Si-NDST1 caused the decreased level of phosphorylated AKT in hypoxia-induced H9C2 cells. Moreover, pcDNA-NDST1 increased the level of phosphorylated AKT in hypoxia-induced H9C2 cells, and pcDNA-NULP1 inhibited the decrease of phosphorylated AKT level induced by pcDNA-NDST1. Hypoxia treatment increased IL-6 and TNF-α levels in the hypoxia-induced H9C2 cells (Fig. 6B). The increased NDST1 promoted the expressions of IL-6 and TNF-α and the increased NULP1 inhibited the change of IL-6 and TNF-α induced by the increased NDST1 in the hypoxia-induced H9C2 cells. Those results showed that NDST1/NULP1 might regulate the phosphorylation of AKT and the secretion of inflammatory factors in hypoxia-induced H9C2 cells.

Discussion

The present study reported that increased NDST1 and decreased NULP1 were found in the heart tissue of HPH-induced RVH rats. *In vitro* tests showed that inhibiting NDST1 expression enhanced cell viability, reduced cell apoptosis, alleviated cardiomyocyte hypertrophy, decreased inflammation, and increased phosphorylated AKT level and over-expression of NDST1 had opposing effects on those aspects; NULP1 reversed the effects of NDST1 on those regulations. Our study confirmed that inhibition of the NDST1/NULP1 pathway might contribute to attenuating RVH induced by HPH.

At present, there are many studies on the pathogenesis of myocardial hypertrophy, mainly focusing on myocardial pressure overload, myocardial apoptosis, vascular remod-

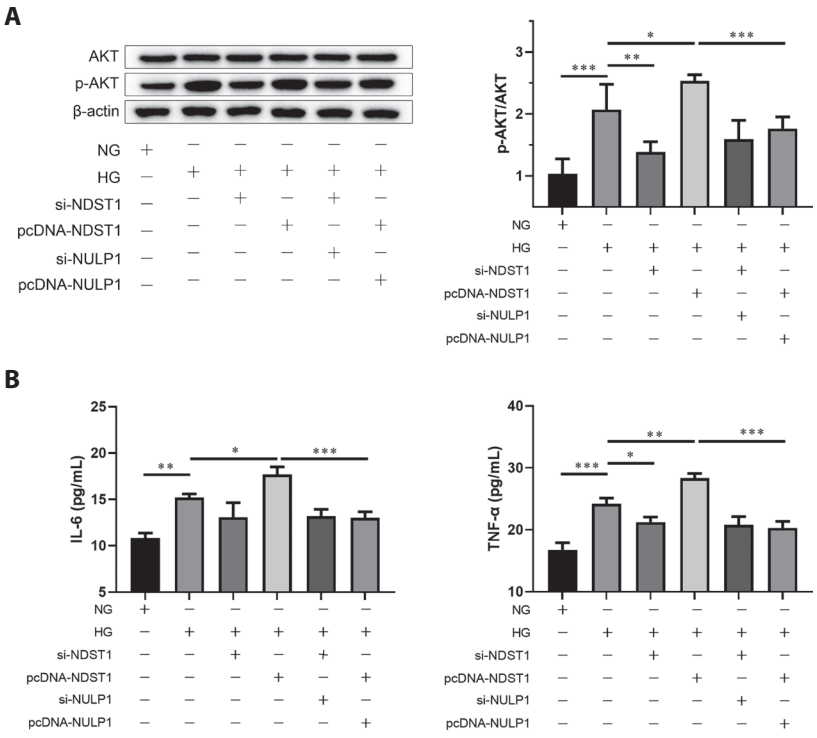

Figure 6. NDST1/NULP1 regulated the phosphorylation of AKT and the secretion of inflammatory factors in hypoxia-induced H9C2 cells. **A.** Western blot detected for phosphorylated AKT. **B.** The inflammatory factors were detected by ELISA. * $p < 0.05$, ** $p < 0.01$, *** $p < 0.001$. For abbreviations, see Figure 1.

eling, oxidative stress, inflammatory response, and so on (Gong et al. 2013; Lyon et al. 2015; García-Redondo et al. 2016; Shimizu and Minamino 2016; Facundo et al. 2017; Chen et al. 2019). In our study, we found that RVH induced by HPH increased IL-6 and TNF-α levels in the heart tissue. Those indicated that RVH induced by HPH could induce heart inflammation and increased the damage with prolonged hypoxia.

A study shows that NDST1 is one of the differentially up-regulated genes in cells after hypoxia (Saygin et al. 2020). In the present study, we observed a high expression of NDST1 in RVH rats. And *in vitro* assays showed that the less expression of NDST1 inhibited hypertrophy and the high expression of NDST1 had the opposite effect on these cell properties. Thus, our study suggested that suppression of NDST1 expression could mitigate cardiomyocyte hypertrophy in hypoxia-induced H9C2 cells.

NULP1 is a negative regulator of cardiac hypertrophy, which is inactivated by the direct interaction with NFAT3 (Zhang et al. 2020). In our study, we found a low expression of NULP1 in RVH rats. Our *in vitro* assays provided evidence that the functional effects of NDST1 alteration on cardiomyocyte hypertrophy could be reversed by NULP1 modulation in hypoxia-induced H9C2 cells, NDST1 and NULP1 were negatively associated. Interestingly, up-regulated NDST1 reduced NULP1 expression and down-regulated NDST1 increased NULP1 expression, further indicating that NDST1 might be an upstream regulatory factor of NULP1. However, there was a lack of correlation reported, and more in-depth studies are needed in the future.

During the development of myocardial hypertrophy, cardiomyocyte apoptosis plays an important role (Wu et al. 2021), and cardiomyocyte apoptosis is a crucial factor leading to myocardial dysfunction (Liu et al. 2021). Studies have shown that a large number of inflammatory factors, such as TNF-α, IL-6, and so on, participate in ventricular apoptosis in myocardial hypertrophy (Haudek et al. 2007; Gullestad et al. 2012). Activating the AKT pathway, such as PI3K/Akt signaling pathway, could induce cardiomyocyte hypertrophy (Xie et al. 2015; Zhong et al. 2020). It has been proved that the activated AKT pathway exerted anti-apoptotic effects to play a cardioprotective effect in myocardial injury induced by myocardial ischemia or sepsis (Matsui et al. 2001, 2002; DeBosch et al. 2006; Roberts et al. 2013; Yu et al. 2019). Interestingly, in our study, it was observed the increased AKT phosphorylation and cardiomyocyte apoptosis in hypoxia-induced H9C2 cells. Through searching, we found that AKT pathway was activated in myocardial hypertrophy (Guan et al. 2019), agreeing with our findings. Therefore, the AKT pathway might have different modulatory effects on cardiomyocyte apoptosis in different types of myocardial injury or not be involved in the regulation of cardiomyocyte apoptosis in hypoxia-induced cardiac hypertrophy. Moreover, AKT phosphorylation also had positive correlations with NDST1 level, when increased NDST1 level, AKT phosphorylation level was increased; and when decreased NDST1 level, AKT

phosphorylation level was decreased. Similarly, NULP1 regulation reversed the change in AKT phosphorylation levels induced by NDST1. Therefore, those data furthermore demonstrated that the regulation of NDST1/NULP1 in cardiac hypertrophy induced by hypoxia was related to AKT phosphorylation.

In conclusion, our study confirmed that inhibition of the NDST1/NULP1 pathway contributed to attenuating RVH induced by HPH, and the mechanism may be reducing inflammation, cardiomyocyte apoptosis, and AKT phosphorylation. However, there are fewer studies related to NDST1/NULP1 pathway in RVH, so a larger study is required to further address this issue to verify the efficacy and safety, including *in vitro* and *in vivo* assays.

Data availability. The initial data used to support the findings of this study are available from the corresponding author upon request.

Conflicts of interest. There are no conflicts of interest.

Authors contributions. HS and JL conceived and the study, HS, JL, YS, FL, MZ, JL, and MS conducted the experiments, HS and JL analyzed the data, HS and JL wrote the manuscript, all authors read and approved the final version.

Funding. This work was supported by the Province Natural Science Foundation of Qinghai (2020-ZJ-777).

Reference

Cai Z, Wang Y, Yu W, Xiao J, Li Y, Liu L, Zhu C, Tan K, Deng Y, Yuan W, et al. (2006): hnulp1, a basic helix-loop-helix protein with a novel transcriptional repressive domain, inhibits transcriptional activity of serum response factor. Biochem. Biophys. Res. Commun. **343,** 973-981 https://doi.org/10.1016/j.bbrc.2006.02.187

Cardiff RD, Miller CH, Munn RJ (2014): Manual hematoxylin and eosin staining of mouse tissue sections. Cold Spring Harbor protocols. **2014,** 655-658 https://doi.org/10.1101/pdb.prot073411

Chen F, Wang H, Zhao J, Yan J, Meng H, Zhan H, Chen L, Yuan L (2019): Grape seed proanthocyanidin inhibits monocrotaline-induced pulmonary arterial hypertension via attenuating inflammation: in vivo and in vitro studies. J. Nutr. Biochem. **67,** 72-77 https://doi.org/10.1016/j.jnutbio.2019.01.013

DeBosch B, Sambandam N, Weinheimer C, Courtois M, Muslin AJ (2006): Akt2 regulates cardiac metabolism and cardiomyocyte survival. J. Biol. Chem. **281,** 32841-32851 https://doi.org/10.1074/jbc.M513087200

Facundo H, Brainard RE, Caldas FRL, Lucas AMB (2017): Mitochondria and cardiac hypertrophy. Adv. Exp. Med. Biol. **982,** 203-226 https://doi.org/10.1007/978-3-319-55330-6_11

Fang W-J, Wang C-J, He Y, Zhou Y-L, Peng X-D, Liu S-K (2018): Resveratrol alleviates diabetic cardiomyopathy in rats by improving mitochondrial function through PGC-1α deacetylation. Acta Pharmacol. Sin. **39,** 59-73 https://doi.org/10.1038/aps.2017.50

García-Redondo AB, Aguado A, Briones AM, Salaices M (2016): NADPH oxidases and vascular remodeling in cardiovascular diseases. Pharmacol. Res. **114,** 110-120 https://doi.org/10.1016/j.phrs.2016.10.015

Gong W, Duan Q, Cai Z, Chen C, Ni L, Yan M, Wang X, Cianflone K, Wang DW (2013): Chronic inhibition of cGMP-specific phosphodiesterase 5 suppresses endoplasmic reticulum stress in heart failure. British J. Pharmacol. **170,** 1396-1409 https://doi.org/10.1111/bph.12346

Gourlay CW, Carpp LN, Timpson P, Winder SJ, Ayscough KR (2004): A role for the actin cytoskeleton in cell death and aging in yeast. J. Cell Biol. **164,** 803-809 https://doi.org/10.1083/jcb.200310148

Guan P, Sun Z-M, Wang N, Zhou J, Luo L-F, Zhao Y-S, Ji E-S (2019): Resveratrol prevents chronic intermittent hypoxia-induced cardiac hypertrophy by targeting the PI3K/AKT/mTOR pathway. Life Sci. **233,** 116748 https://doi.org/10.1016/j.lfs.2019.116748

Gullestad L, Ueland T, Vinge LE, Finsen A, Yndestad A, Aukrust P (2012): Inflammatory cytokines in heart failure: mediators and markers. Cardiology **122,** 23-35 https://doi.org/10.1159/000338166

Haudek SB, Taffet GE, Schneider MD, Mann DL (2007): TNF provokes cardiomyocyte apoptosis and cardiac remodeling through activation of multiple cell death pathways. J. Clin. Invest. **117,** 2692-2701 https://doi.org/10.1172/JCI29134

Lachtermacher S, Esporcatte BL, Montalvão F, Costa PC, Rodrigues DC, Belem L, Rabischoffisky A, Faria Neto HC, Vasconcellos R, Iacobas S, et al. (2010): Cardiac gene expression and systemic cytokine profile are complementary in a murine model of post-ischemic heart failure. Brazilian J. Med. Biol. Res. **43,** 377-389 https://doi.org/10.1590/S0100-879X2010007500014

Li H, Xu C, Li Q, Gao X, Sugano E, Tomita H, Yang L, Shi S (2017): Thioredoxin 2 offers protection against mitochondrial oxidative stress in H9c2 cells and against myocardial hypertrophy induced by hyperglycemia. Int. J. Mol. Sci. **18,** 1958 https://doi.org/10.3390/ijms18091958

Liu L, Yan M, Yang R, Qin X, Chen L, Li L, Si J, Li X, Ma K (2021): Adiponectin attenuates lipopolysaccharide-induced apoptosis by regulating the Cx43/PI3K/AKT Pathway. Front. Pharmacol. **12,** 644225 https://doi.org/10.3389/fphar.2021.644225

Lyon RC, Zanella F, Omens JH, Sheikh F (2015): Mechanotransduction in cardiac hypertrophy and failure. Circul. Res. **116,** 1462-1476 https://doi.org/10.1161/CIRCRESAHA.116.304937

Matsui T, Li L, Wu JC, Cook SA, Nagoshi T, Picard MH, Liao R, Rosenzweig A (2002): Phenotypic spectrum caused by transgenic overexpression of activated Akt in the heart. J. Biol. Chem. **277,** 22896-22901 https://doi.org/10.1074/jbc.M200347200

Matsui T, Tao J, del Monte F, Lee KH, Li L, Picard M, Force TL, Franke TF, Hajjar RJ, Rosenzweig A (2001): Akt activation

preserves cardiac function and prevents injury after transient cardiac ischemia in vivo. Circulation **104,** 330-335 https://doi.org/10.1161/01.CIR.104.3.330

Roberts DJ, Tan-Sah VP, Smith JM, Miyamoto S (2013): Akt phosphorylates HK-II at Thr-473 and increases mitochondrial HK-II association to protect cardiomyocytes. J. Biol. Chem. **288,** 23798-23806 https://doi.org/10.1074/jbc.M113.482026

Rops AL, Loeven MA, van Gemst JJ, Eversen I, Van Wijk XM, Dijkman HB, van Kuppevelt TH, Berden JH, Rabelink TJ, Esko JD, van der Vlag J (2014): Modulation of heparan sulfate in the glomerular endothelial glycocalyx decreases leukocyte influx during experimental glomerulonephritis. Kidney Int. **86,** 932-942 https://doi.org/10.1038/ki.2014.115

Saygin D, Tabib T, Bittar HET, Valenzi E, Sembrat J, Chan SY, Rojas M, Lafyatis R (2020): Transcriptional profiling of lung cell populations in idiopathic pulmonary arterial hypertension. Pulm Circ. **10,** 1-15 https://doi.org/10.1177/2045894020908782

Shimizu I, Minamino T (2016): Physiological and pathological cardiac hypertrophy. J. Mol. Cell. Cardiol. **97,** 245-262 https://doi.org/10.1016/j.yjmcc.2016.06.001

Steen H, Lindholm D (2008): Nuclear localized protein-1 (Nulp1): increases cell death of human osteosarcoma cells and binds the X-linked inhibitor of apoptosis protein. Biochem. Biophys. Res. Com. **366,** 432-437 https://doi.org/10.1016/j.bbrc.2007.11.146

Tyser RC, Miranda AM, Chen C-M, Davidson SM, Srinivas S, Riley PR (2016): Calcium handling precedes cardiac differentiation to initiate the first heartbeat. Elife **5,** e17113 https://doi.org/10.7554/eLife.17113

Wang L, Fuster M, Sriramarao P, Esko JD (2005): Endothelial heparan sulfate deficiency impairs L-selectin- and chemokine-mediated neutrophil trafficking during inflammatory responses. Nat. Immunol. **6,** 902-910 https://doi.org/10.1038/ni1233

Wu X, Wei M, Zhang H, Fan X, Ma X, Liu J, Xue M (2021): The protective effect of aspirin against myocardial hypertrophy in rats. BioMed. Res. Int. **2021,** 2043415 https://doi.org/10.1155/2021/2043415

Xie F, Liu W, Feng F, Li X, He L, Lv D, Qin X, Li L, Li L, Chen L (2015): Apelin-13 promotes cardiomyocyte hypertrophy via PI3K-Akt-ERK1/2-p70S6K and PI3K-induced autophagy. Acta Biochim. Biophys. Sin. (Shanghai) **47,** 969-980 https://doi.org/10.1093/abbs/gmv111

Yu T, Liu D, Gao M, Yang P, Zhang M, Song F, Zhang X, Liu Y (2019): Dexmedetomidine prevents septic myocardial dysfunction in rats via activation of α7nAChR and PI3K/Akt- mediated autophagy. Biomed. Pharmacother. **120,** 109231 https://doi.org/10.1016/j.biopha.2019.109231

Zangiabadi A, De Pasquale CG, Sajkov D (2014): Pulmonary hypertension and right heart dysfunction in chronic lung disease. Biomed. Res. Int. **2014,** 739674 https://doi.org/10.1155/2014/739674

Zeng C, Liang B, Jiang R, Shi Y, Du Y (2017): Protein kinase C isozyme expression in right ventricular hypertrophy induced by pulmonary hypertension in chronically hypoxic rats. Mol. Med. Rep. **16,** 3833-3840 https://doi.org/10.3892/mmr.2017.7098

Zhang X, Lei F, Wang X-M, Deng K-Q, Ji Y-X, Zhang Y, Li H, Zhang X-D, Lu Z, Zhang P (2020): NULP1 alleviates cardiac hypertrophy by suppressing NFAT3 transcriptional activity. J. Am. Heart Assoc. **9,** e016419 https://doi.org/10.1161/JAHA.120.016419

Zhong S, Guo H, Wang H, Xing D, Lu T, Yang J, Wang C (2020): Apelin-13 alleviated cardiac fibrosis via inhibiting the PI3K/Akt pathway to attenuate oxidative stress in rats with myocardial infarction-induced heart failure. Biosci. Rep. **40,** BSR20200040 https://doi.org/10.1042/BSR20200040

Received: March 2, 2022
Final version accepted: June 1, 2022

doi: 10.4149/gpb_2022032

Supplementary Material

The role and mechanism of NDST1/NULP1 regulating right ventricular hypertrophy in hypoxic pulmonary hypertension

Haixia Sun[1,*], Junling Liu[2,*], Yuxin Su[1], Fang Li[1], Mingyue Zhang[1], Jia Li[1] and Meiling Song[3]

[1] *Qinghai Provincial People's Hospital, Xining, Qinghai, China*
[2] *Xining Hospital of Traditional Chinese Medicine, Xining, Qinghai, China*
[3] *Medical College of Qinghai University, Xining, Qinghai, China*

Supplementary figure

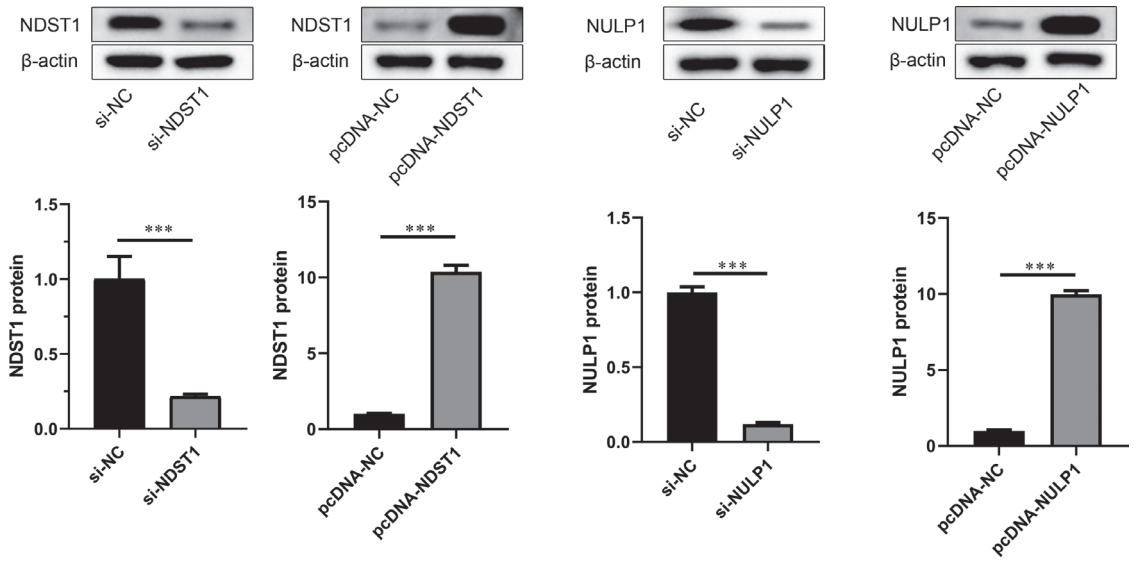

Figure S1. Transfection results.